551.509.324: 551.509.313

NEW ZEALAND METEOROLOGICAL SERVICE

TECHNICAL NOTE 203

THE OBJECTIVE PREDICTION OF CLOUD AND PRECIPITATION

A.J. May and J.W. Kidson

Issued for limited distribution by:

The Director,
New Zealand Meteorological Service,
P.O. Box 722,
WELLINGTON.

21 October, 1971.

NEW ZEALAND METEOROLOGICAL SERVICE

THE OBJECTIVE PREDICTION OF CLOUD AND PRECIPITATION

A.J. May and J.W. Kidson

Abstract

An objective method for predicting cloud cover and precipitation amounts is described which uses a vertically integrated moisture parameter closely related to the mean relative humidity in the 1000-500 mb layer. The model is designed to be run in parallel with a baroclinic prediction scheme. To illustrate the type of results obtained, the 24 hour computer predictions for the Australia - N.Z. region based on radiosonde and satellite data for 00 GMT 2nd January 1971 are discussed.

Introduction

Numerical predictions of circulation patterns are already routinely available to the forecaster in this country and are likely to become of increasing importance as the observing network and the sophistication of the forecasting model improve. Up to the present however no attempt has been made to obtain the associated patterns of cloud and precipitation. The intention here has been firstly to provide objective forecasts of humidity elements for the guidance of the manual forecaster and secondly to obtain estimates of latent heat release for inclusion in the 5-level baroclinic model currently being developed.

For our first attempt we have chosen a very simple scheme which nevertheless gives quite encouraging results. Multi-level models are generally preferred for this purpose overseas as they depict more accurately the complex 3-dimensional condensation process but quite successful predictions may be made by considering only the mean relative humidity in a vertical column throughout the depth of the troposphere. Statistical relations enable the precipitation rate and cloud cover to be derived from the forecast values of mean relative humidity.

The Prediction Model

The prediction model which we have used is based on the work of Younkin et al (1965) and a brief outline of their method is presented here together with our modifications.

The water vapour content of a vertical column extending through the depth of the atmosphere is known as the precipitable water, W, and is defined by

$$W = \frac{1}{g}\int_0^{\tilde{\pi}} q\, dp = \frac{\tilde{\pi}}{g}\int_0^1 q\, d\sigma \qquad \ldots (1)$$

where $\tilde{\pi}$ is the surface pressure, $\sigma = p/\tilde{\pi}$ and q is the specific humidity. In practice 500 mb can be used as an effective upper boundary. If there is no loss or gain of water from the column and the principle of mass conservation is used, a prediction equation for the precipitable water can be derived (Younkin et al, loc. cit).

$$\begin{aligned}\frac{\partial W}{\partial t} &= \frac{1}{g}\int_0^1 \nabla\cdot(\tilde{\pi} q \mathbb{V})\, d\sigma \\ &= \frac{\tilde{\pi}}{g}\int_0^1 (-\mathbb{V}\cdot\nabla q)\, d\sigma + \frac{\tilde{\pi}}{g}\int_0^1 (-q\nabla\cdot\mathbb{V})\, d\sigma \\ &\quad + \frac{1}{g}\int_0^1 (-q\mathbb{V}\cdot\nabla\tilde{\pi})\, d\sigma\end{aligned} \qquad \ldots (2)$$

This equation expresses the local change of the precipitable water in terms of advection of specific humidity, horizontal divergence in the wind field and variation in the surface elevation. If we assume that q, $\mathbb{V}$ and $\nabla\cdot\mathbb{V}$ can be modelled in the vertical as functions of the pressure (in accordance with observational evidence), equation (2) may be rewritten in the form

$$\frac{\partial W}{\partial t} = -\mathbb{V}_*\cdot\nabla W - K_1 W\omega_m + K_2 W\sigma_m \mathbb{V}_5\cdot\nabla\tilde{\pi} \qquad \ldots (3)$$

where K_1 and K_2 are constants derived from station data, $\mathbb{V}_5$ is the 500 mb wind and $\mathbb{V}_*$ an empirical steering flow derived from the 1000 and 500 mb winds, and m indicates the level where

$$\mathbb{V}_m = \overline{\mathbb{V}} = \int_0^1 \mathbb{V}\, d\sigma$$

A more convenient form of this equation uses the saturation thickness h_s (Swayne, 1956) which is the depth of a column having a mean relative humidity of 0.7, a moist adiabatic lapse rate and which contains the observed precipitable water. The factor 0.7 is an empirical correction allowing for a low bias in radiosonde observations but is not an essential part of the following theory. Its inclusion only affects the results in that cloud and precipitation occur when the mean relative humidity as measured by radiosonde over the 1000-500 mb layer is closer to 1.0. Figure 1 shows the relation between precipitable water and saturation thickness where the least-squares regression line has the equation

$$h_s = 323 \ln W + 4447 \qquad \ldots (4)$$

A similar relation applies between the observed 1000-500 mb thickness, h, and the corresponding saturation precipitable water.

The degree of saturation can now be expressed by the saturation deficit, h_d:

$$h_d = h - h_s \qquad \ldots (5)$$

so that saturation occurs when the saturation deficit drops to zero. A prediction equation for the saturation deficit can be derived from equation (3) by assuming that processes are adiabatic and the direction of the vertical wind shear is constant within the 1000-500 mb layer.

$$\frac{\partial h_d}{\partial t} = \frac{Cf}{g} \frac{\partial}{\partial t} (\psi_5 - \psi_0)$$

$$- J\left[\psi_*, hd + (P-A) - \frac{Cf}{g}(\psi_5 - \psi_0)\right] \qquad \ldots (6)$$

where ψ is the stream function defining

$$\mathbb{V} = \mathbb{K} \times \nabla \psi$$

and the subscript $_0$ indicates the 1000 mb level.
C is a constant empirically derived from observations and P - A is an orographic effect applied to the saturation deficit to compensate for surface pressures differing from 1000 mb. The values taken are given below:

π	1000	950	900	850	mb
P - A	0	4	8	12	gpm

Equation (6) differs from the corresponding equation of Younkin et al in that C is a constant chosen to give optimum predictions and that we are using a stream function rather than a geopotential field to represent the basic flow. It relates the local change in saturation deficit to changes in the 1000-500 mb thickness, advection and orographic effects. Orographic ascent for example results in an increase in P - A and a corresponding decrease in saturation deficit.

It was found that using equation (5) directly to obtain an analysis of the saturation deficit was not practicable. The 1000-500 mb thickness and the saturation thickness are large quantities of similar magnitude, both are strongly latitude-dependent and their small difference (the saturation deficit) is subject to large errors. As the mean relative humidity of the layer, $\overline{RH}$, is the ratio of the observed to the saturation precipitable water, applying equation (4) to the definition of the saturation deficit leads to

$$h_d = -323 \ln \overline{RH} \qquad \ldots (7)$$

The mean relative humidity is an easier quantity to work with as it is not subject to the errors discussed above and is more readily and accurately determined from available data. Input and output from the program are therefore in the form of relative humidity fields with conversion to the saturation deficit for computation of the forecast.

In the numerical scheme using the National Weather Forecasting Centre (N.W.F.C.) 800 point grid a centred time step formula is used to obtain the forecast saturation deficit:

$$h_d^{\nu+1} = h_d^{\nu-1} + 2\,\Delta t \left.\frac{\partial h_d}{\partial t}\right|^{\nu} \qquad \ldots (8)$$

where the superscript ν denotes the time step and Δt is the length of the time step, currently 36 minutes. At present the water vapour prediction scheme is run separately from the baroclinic model which provides on magnetic tape the sets of 1000 and 500 mb stream functions and their time derivatives required at each time step. It is intended to combine the two schemes shortly so that the release of latent heat can be fed back into the baroclinic model.

Data Extraction

Two sources of data are used at present to obtain the initial mean relative humidity field. Firstly, radiosonde observations provide a series of readings of the dewpoint, T_d, at significant levels from which the specific humidity can be calculated (Haurwitz, 1941):

$$q = \frac{K}{P} \cdot 10^{\left(\frac{aT_d}{b+T_d}\right)} \qquad \ldots (9)$$

where k is a constant and a and b are coefficients depending on whether saturation is with respect to water or ice. Numerical integration following equation (1) gives the precipitable water. The observed thickness can be converted to the saturation precipitable water using equation (4) and hence the mean relative humidity computed.

These observations are fairly easily extracted and provide the basic observing network over land. We note however that because of the spot nature of the observations they reflect the mesoscale variations in the circulation pattern and the relative humidities may differ by as much as 0.3 from the value characteristic of the air mass around the station. The absence of radiosonde data over the oceans would be a severe limitation on the accuracy of the forecasts but for satellite photographs which cover the entire prediction area and furnish a reasonably accurate subjective humidity field in these areas.

The relationship between observed cloud on satellite photographs and humidity was investigated soon after the prediction scheme was published (Thompson and West, 1967) and it was found that a good correlation existed, modified by latitudinal, seasonal and maritime-continental variations. The system of classification used at present (Smigielski and Mace, 1970) depends on accurately assessing cloud amount, type and vertical development. With this knowledge an estimate of the mean relative humidity can be made to within about 0.1. Although it is difficult to check the accuracy of these estimates the radiosonde-derived data agree reasonably well where comparisons are possible.

The main classifications according to the mean relative humidity are given below. It must be remembered that these classifications apply on a synoptic scale and wide variations can occur within an area assigned a single humidity value.

Mean Relative Humidity	Cloud Type
Greater than 0.8	(a) Multi-layered cloud bands extending to the cirrus level.
	(b) At centre of bright bands (active fronts), 0.9.
	(c) Inactive frontal bands and areas of cumulonimbus activity.

0.6 - 0.8	(a) Broken frontal bands, 0.7 for entire region. (b) Areas covered with middle cloud, other stratus, cumulus, cirrus present. (c) Frontal bands of low and middle cloud south of jet stream. (d) Cumuliform cloud with vorticity maximum, 0.8 at centre.
0.4 - 0.6	(a) Scattered to broken cumuliform. (b) Open cell cumuliform with cold advection over warmer seas. (c) Continuous or broken cumuliform or stratiform (no vertical development) in a cold outbreak, 0.4 - 0.5.
Less than 0.4	(a) Clear areas or cirriform only. (b) Widely scattered cumuliform (no vertical development). (c) Low level stratus or strato-cumulus.

For use by the prediction scheme observations from these two sources are interpolated to the 800 point N.W.F.C. grid using the Cressman objective analysis technique (Cressman, 1959). This method employs a series of scans with a decreasing influence radius in which each grid point value is adjusted to best fit the surrounding station values. In an operational scheme the initial guess field would be the forecast grid point values but at present a latitudinal trend in the mean relative humidity is constructed from the observations. The parameters used in the analysis program are given below.

Scan	Radius (grid units)	Guess-weight	Smoothing
1	6	5	0.2
2	5	1	0
3	3	0	0
4	2	0	0.4

The guess-weight is the relative weighting of the guess field to the observations and the large value in the first scan helps maintain the latitudinal trend in areas of few observations. The amount of five-point smoothing can be varied between 0 and 1. Provision is also made during each pass for the rejection of observations with unacceptably large anomalies.

Derivation of Cloud Cover and Rainfall

The climatological records for 1966-1970 (Nandi, Auckland, Christchurch and Invercargill) were studied and frequency tables prepared comparing the radiosonde-derived humidity observations with the corresponding total cloud cover and hourly rainfall. Although a fair amount of scatter was encountered, resulting from meso and smaller-scale variations, the mean cloud cover and hourly rainfall showed a good correlation with the humidity. Thus, by deriving statistical relationships, it is possible to obtain values for the cloud cover and rainfall from the forecast humidity field.

The relation between total cloud cover in eighths, C, and the mean relative humidity for the four stations is shown in Fig. 2. Least-squares regression lines are drawn and it can be seen that the statistical relation is approximately linear. Some of the extreme points (above 0.85 or below 0.5 humidity) are unreliable due to lack of data. There is some evidence of a latitudinal trend which can be seen more easily in the regression equations:

Nandi (17.8°S)	C	=	10.8 $\overline{RH}$	-	1.7
Auckland (37.0°S)	C	=	10.2 $\overline{RH}$	-	1.4
Christchurch (43.5°S)	C	=	10.5 $\overline{RH}$	-	0.71
Invercargill (46.4°S)	C	=	9.47 $\overline{RH}$	-	0.21

but more data will be needed before it is known whether this trend is significant and can be included in the prediction scheme. At present the cloud cover predictions are simply divided into groups:

$\overline{RH}$	C
Less than 0.45	clear (0,1 eighths)
0.45 to less than 0.55	scattered (2,3,4 eighths)
0.55 to less than 0.70	broken (5,6 eighths)
0.70 or greater	overcast (7,8 eighths)

With the existing accurancy of the humidity forecast a finer resolution of the cloud cover cannot be justified.

Figure 3 shows the mean relative humidity-rainfall rate data for the four stations with least-squares regression lines drawn. The statistical relation in this case is approximately exponential with a latitudinal trend again evident in the diagram and the regression equations:

Nandi (17.8°S)	$\ln r = 26.4\ \overline{RH} - 23.6$
Auckland (37.0°S)	$\ln r = 16.2\ \overline{RH} - 14.5$
Christchurch (43.5°S)	$\ln r = 15.6\ \overline{RH} - 13.5$
Invercargill (46.4°S)	$\ln r = 10.5\ \overline{RH} - 9.60$

where r is the rainfall rate in mm per 36 minutes (the time-step length used in the prediction program). The data for Nandi are probably less reliable than for the other stations due to lack of observations. Here, as in the case of the cloud cover more data will be needed before including a latitudinal trend. The regression equation used at present was obtained by combining all the New Zealand data to give

$$\ln r = 13.8\ \overline{RH} - 12.3$$

By determining the rainfall rate at each time step in the prediction program and accumulating these fields a prediction of the total rainfall during the forecast period can be made. The rainfall rate is also used to modify the humidity forecast at each time step for the precipitable water is reduced by the predicted rainfall and a corresponding reduction is made in the relative humidity. Since the rainfall rate increases exponentially with the humidity until it balances the rate of water vapour convergence, the relative humidity is effectively prevented from rising above 1.0 which sometimes occurred before this loss from the system was taken into account.

Results

The first period used to test the prediction scheme was the 24 hours commencing at 00 GMT on 28 June 1970. The results obtained were encouraging and humidity data were collected for a second period from 2-6 January 1971. During this period a subtropical cyclone developed near 20°S, 165°E and moved south to the west of New Zealand where it merged with a depression which formed near Tasmania and later moved into the Tasman Sea. At 500 mb a large trough moved from Tasmania into the central Tasman, losing intensity as it progressed. Twenty-four hour forecasts of mean relative humidity, rainfall rate and total, and cloud cover were produced with mean errors and standard deviations calculated for the area inside the frame on Fig. 8. We have taken the forecast based on the data for 2 January 1971 to illustrate the type of results obtained by the scheme. Figures 4 and 5 show the ESSA-8 mosaics for 2 and 3 January 1971 (pictures taken at approximately 00 GMT each day, pass numbers

9378-9381 and 9391-9393). During this period the cyclone moved from 22°S, 165°E to 28°S, 167°E.

The initial humidity analysis (Fig. 7) was obtained using the Cressman technique starting with 38 radiosonde-derived observations and 20 observations from the satellite picture; these latter points can be compared with the satellite picture for 2 January 1971 in Fig. 6 which shows most of the data used. (The low Campbell Island observation was rejected by the scheme.)

The machine analysis was compared with a hand analysis showing a mean error of less than 0.01 and a standard deviation of under 0.06. Both of these analyses were used as initial fields for the prediction scheme and there was no significant difference in the results, indicating that the machine analysis was sufficiently reliable to be used directly. The correspondence of the humidity pattern and the observed cloud on the satellite pictures is readily seen and also the relation of the mean relative humidity field to the 1000 mb machine analysis (Fig. 7). We note in each case the high humidity area to the south and east of the cyclone and the dry area to the north and east of the anticyclone. The humidity analysis for 3 January 1971 in Fig. 9 can similarly be compared with the satellite pictures for the same day and also the 1000 mb analysis (Fig. 9). This field was used for verifying the forecast humidity.

If the predicted 1000 mb field in Fig. 8 is compared with the verification 1000 mb analysis it will be seen that the baroclinic scheme failed to predict the southward movement of the cyclone and the central height rose about 100 m instead of remaining constant. However, comparing the forecast mean relative humidity (Fig. 8 also) with the forecast 1000 mb field is more encouraging. The high humidity area is still to the south and east of the cyclone's forecast position and the dry area to the north-east of the high; the humidity is increasing over the trough south of Tasmania. The higher humidity in the north-east on all the maps is due to an almost stationary band of cloud extending south-east from Samoa (off the map). When the humidity forecast was compared with the verification field it was found the mean error was -0.03 and the standard deviation 0.06. The extreme errors in the forecast were +0.19 and -0.22; these occurred where the predicted 1000 mb low and the actual low were placed respectively. Thus an improvement in the 1000 mb forecast should reduce the standard deviation of the forecast error considerably.

The empirical coefficients (see equation (6)) used to produce this forecast were determined using a non-linear optimisation procedure. The resulting equation was:

$$\frac{\partial h_d}{\partial t} = .43\, f/g \frac{\partial}{\partial t}(\Psi_5 - \Psi_0)$$

$$-J\left[.15\Psi_5 + .10\Psi_0,\ h_d + (P-A) - .43\, f/g(\Psi_5 - \Psi_0)\right]$$

Compared with the values for the steering flow suggested by the original paper the weights given the 500 and 1000 mb winds here are rather small and the American data suggest they should total about 1.0. The slow movement of the cyclone during the days used for testing is probably responsible for this, implying a light steering flow and hence reduced coefficients. The American data also suggested that the 1000 mb wind should be the more heavily weighted, leading to an effective moisture steering level at 850-800 mb. The reversal of this may possibly be due to the lack of skill shown in the 1000 mb forecast. The coefficients given above are unlikely however to be any more than the optimum set for this period of 2-6 January 1971 and will be revised when more extensive testing becomes possible.

The initial cloud cover analysis is shown in Fig. 10a. Remembering that the value given is an areal average and a fair amount of scatter can be expected at individual points, there is a good correspondence between the analysis and the satellite pictures for 2 January 1971 and the cloud cover observations plotted on the mean-sea-level analysis.

The main error in the predicted cloud cover (Fig. 10b) is in placing the major band of cloud associated with the cyclone too far west. As in the case of the humidity forecast this is caused by the lack of movement in the 1000 mb forecast.

The predicted rainfall rate for 3 January 1971 is seen in Fig. 11a together with the stations reporting precipitation. Quantitative verification of this forecast is rather difficult but surface observations for 3 January 1971 show precipitation in the areas forecast as well as to the south (Norfolk Island) and the east (Timaru Star at 23°S, 172°E). The predicted total rainfall during the 24 hours is shown in Fig. 11b. Verification of this field is also difficult but examination of the 06, 12, 18, 21 GMT maps for 2 January 1971 show rainfall on all the maps in the areas where it was forecast. Ship reports of continuous moderate rain at 12 and 18 hours in the Tasman Sea south of Norfolk Island and continuous light rain reported at 18 hours at Haast indicate that more rain fell in the Tasman Sea west of New Zealand than forecast. Although the rainfall patterns are affected in the same way as the humidity field by the baroclinic prediction at 1000 mb the results seem reasonable, and a prediction done for a period with significant rainfalls over land would help to check the accuracy of the forecasting scheme.

Conclusions

The results obtained for the second period in January were on the whole encouraging, with reasonably successful forecasts of large scale weather patterns covering an area

of several grid squares (one grid unit is 381 km at 60°S). Clearly no attempt can be made at present to forecast any smaller scale effects and there are obvious limitations to the prediction of narrow frontal rain bands.

It appears that computer analyses of the mean relative humidity are sufficiently accurate to be used without modification as input to the prediction scheme. The need remains however for estimates of the relative humidity over the oceans to be taken manually from satellite pictures to supplement the basic radiosonde network if satisfactory results are to be obtained. In this respect it should be noted that the television satellite coverage during the winter months is rather poor and we will need techniques for deriving the same information from infrared pictures.

The main factor determining the accuracy of the relative humidity predictions appears to be the limited skill shown by the 1000 mb forecasts of the baroclinic model. The humidity forecasts are however dynamically consistent with the predicted flow patterns and any further improvement in their accuracy must therefore await a corresponding improvement in the stream function forecasts. One way this may be brought about is by including the release of latent heat in the baroclinic model and steps are already under way to combine the two prediction schemes for this purpose. In the example of the previous section it is anticipated that the release of latent heat to the south of the cyclone centre will help to maintain its intensity and possibly to increase its southward motion to a more realistic rate.

A more detailed study of the cloud and rainfall rate - humidity relations is needed, especially the latitudinal trends, but little can be done at this stage as stations such as Raoul Island and Campbell Island do not make the hourly rainfall observations required.

The treatment of orographic effects by the model is obviously unsuitable for showing rainfall variations over an area the size of New Zealand. Because of the coarseness of the grid the changes in topography are averaged over quite a large area and the differences in forecast relative humidity on either side of the Southern Alps for example may amount to only a few percent. The manual forecaster is therefore required to make suitable adjustments to the rainfall rate in each area based on the grid square averages forecast by the model. Little more can be done without considerably reducing the grid point spacing but the possibility remains for the development of further statistical relations to predict the rainfall in individual catchments in terms of the forecast wind direction and precipitation rate for the area.

References

Cressman, G.P., 1959: An operational objective analysis system. U.S. Mon. Wea. Rev. 87, 367-374.

Haurwitz, B., 1941: "Dynamic Meteorology". McGraw - Hill Book Co., New York.

Smigielski, F.J. and L.M. Mace, 1970: Estimating mean relative humidity from the surface to 500 mb by use of satellite pictures. ESSA NESCTM 23.

Swayne, W.W., 1956: Quantitative analysis and forecasting of winter rainfall patterns. U.S. Mon. Wea. Rev. 84, 53-65.

Thompson, A.H. and P.W. West, 1967: Use of satellite cloud pictures to estimate average relative humidity below 500 mb with application to the Gulf of Mexico area. U.S. Mon. Wea. Rev. 95, 791-798.

Younkin, R.J., J.A. La Rue, and F. Sanders, 1965: The objective prediction of clouds and precipitation using vertically integrated moisture and adiabatic vertical motions. J. Appl. Meteor. 4, 3-17.

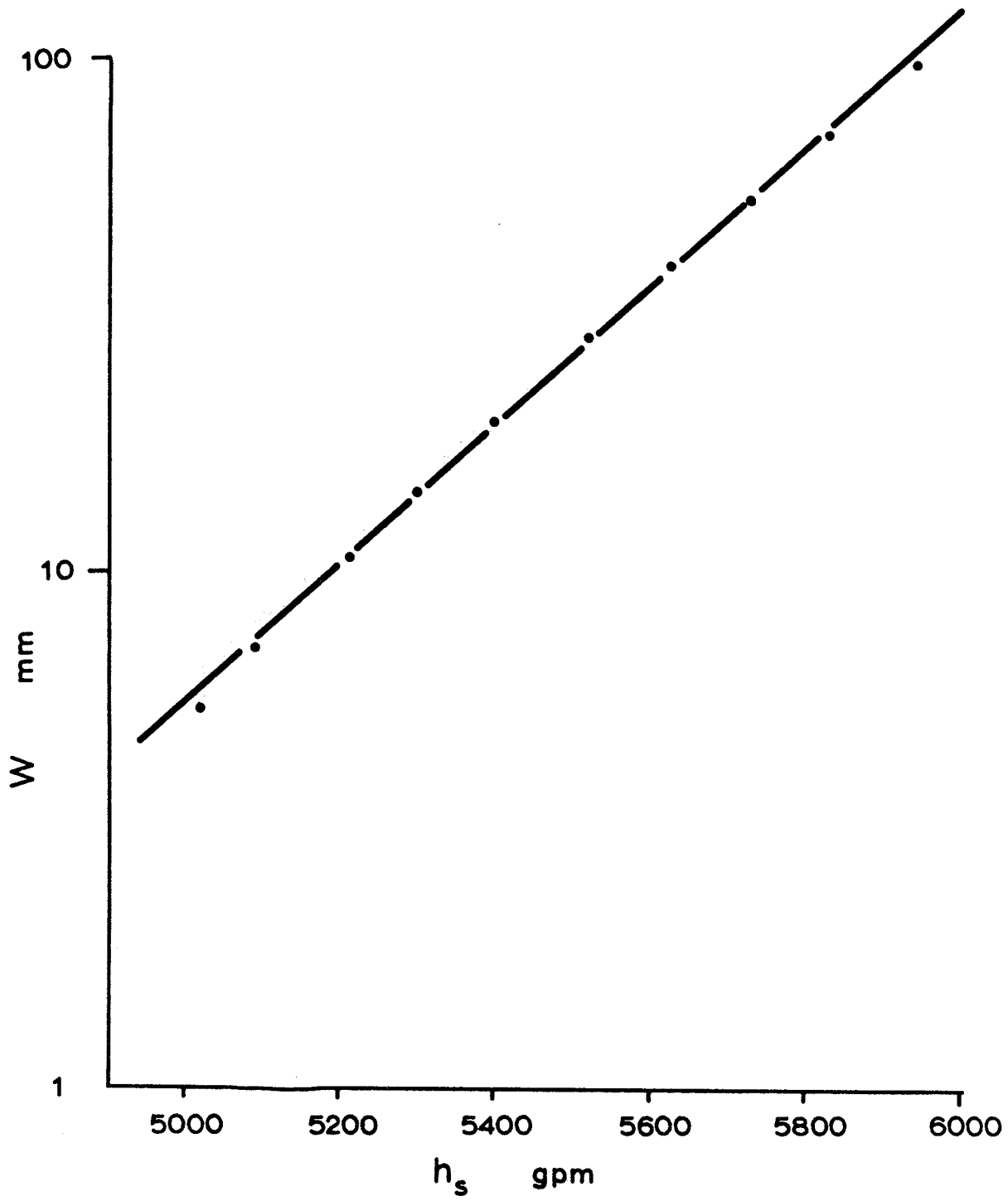

Fig. 1 Relation between precipitable water, W, and saturation thickness, h_s.

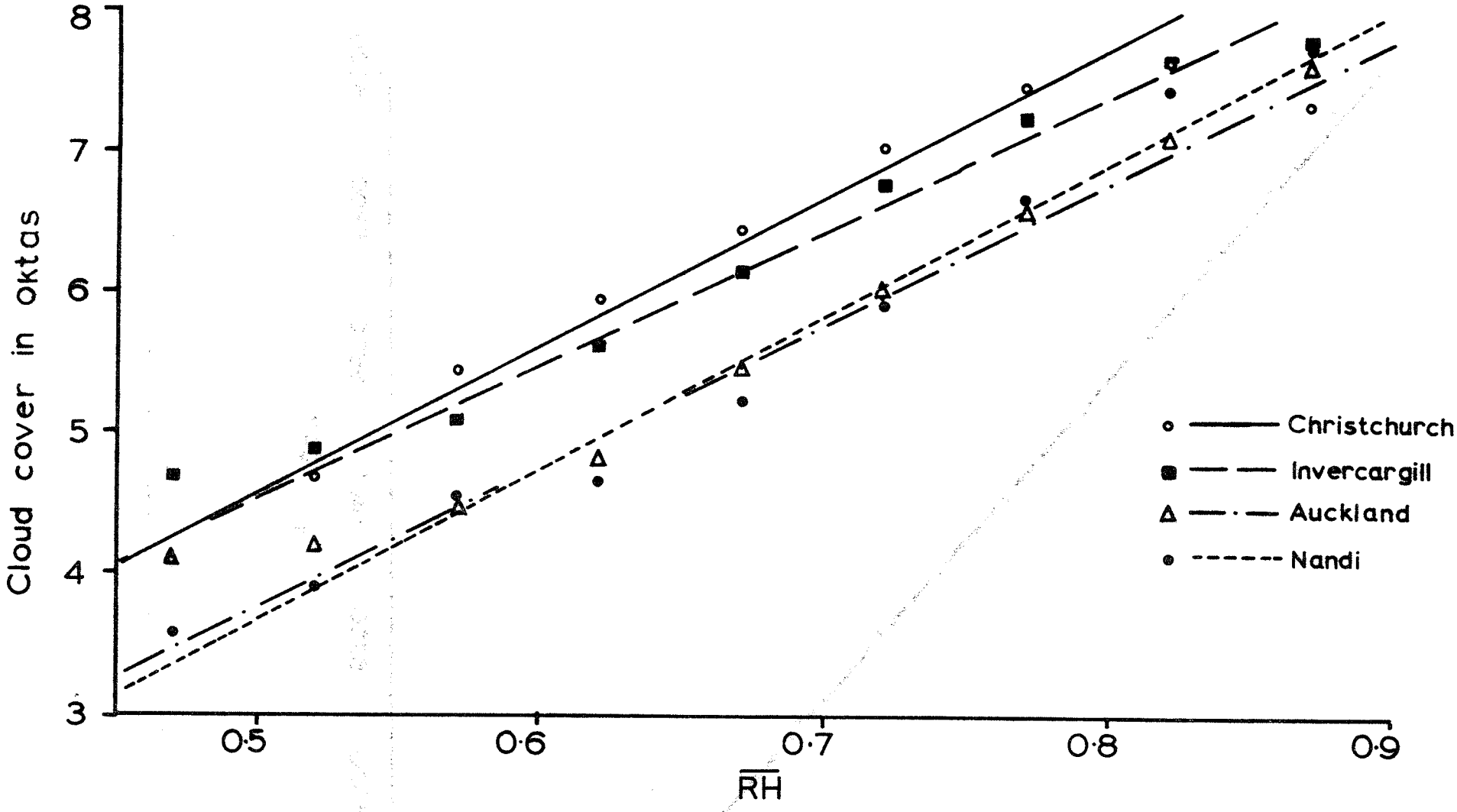

Fig.2 Total cloud cover in oktas as a function of the mean relative humidity at Nandi, Auckland, Christchurch and Invercargill.

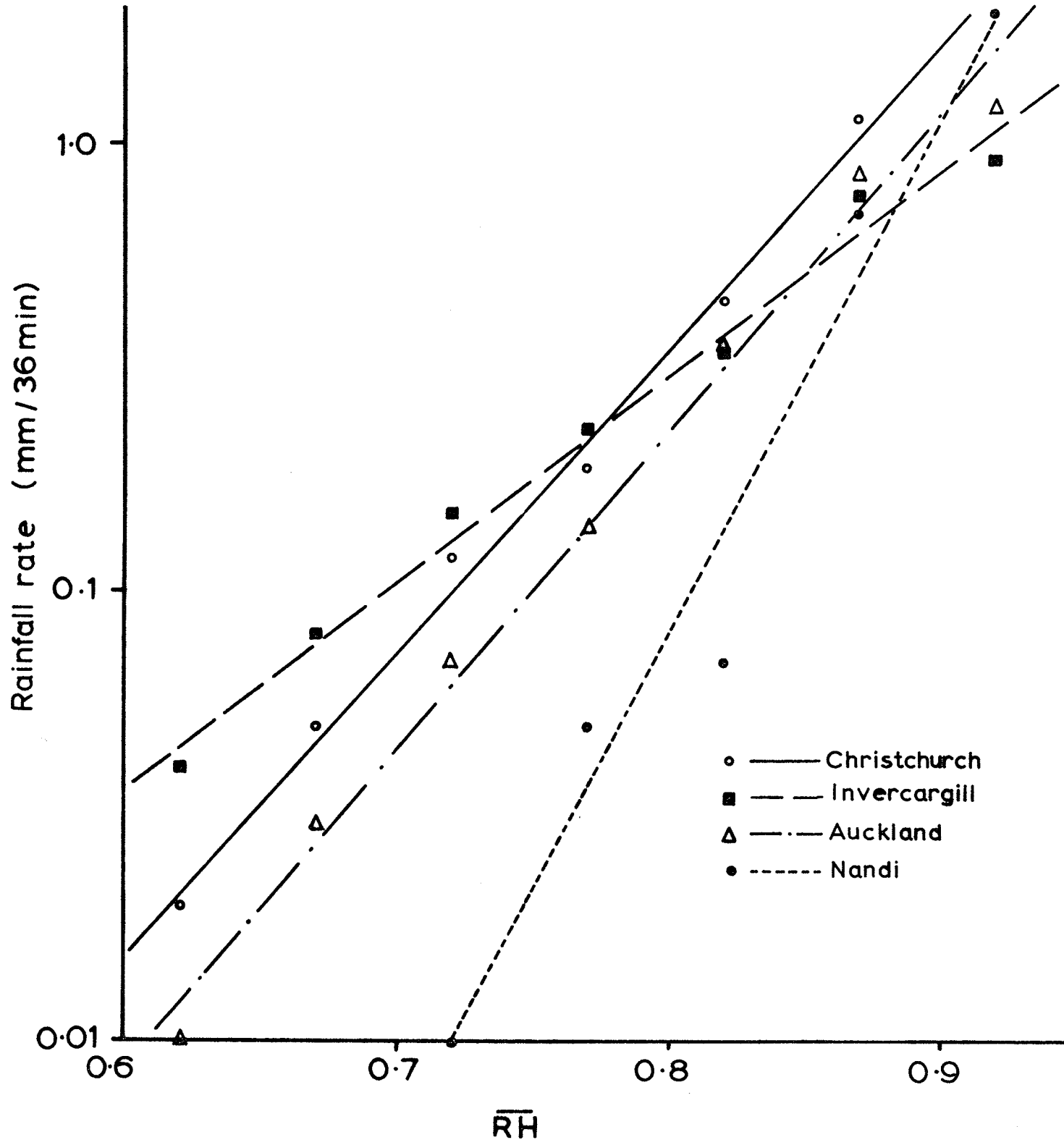

Fig. 3 Rainfall rate as a function of mean relative humidity for Nandi, Auckland, Christchurch and Invercargill.

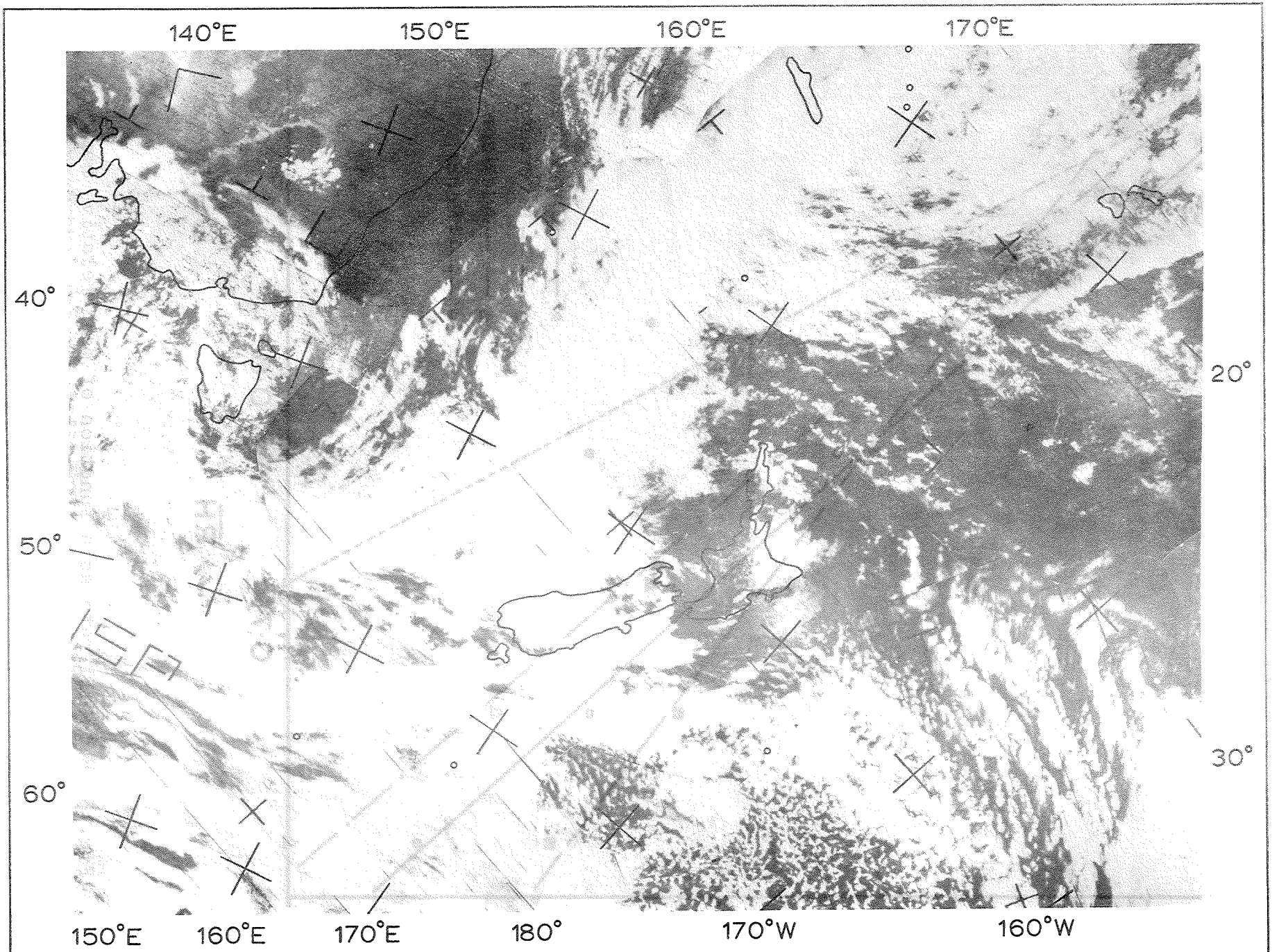

FIGURE 4 : ESSA-8 MOSAIC FOR 2 JANUARY 1971

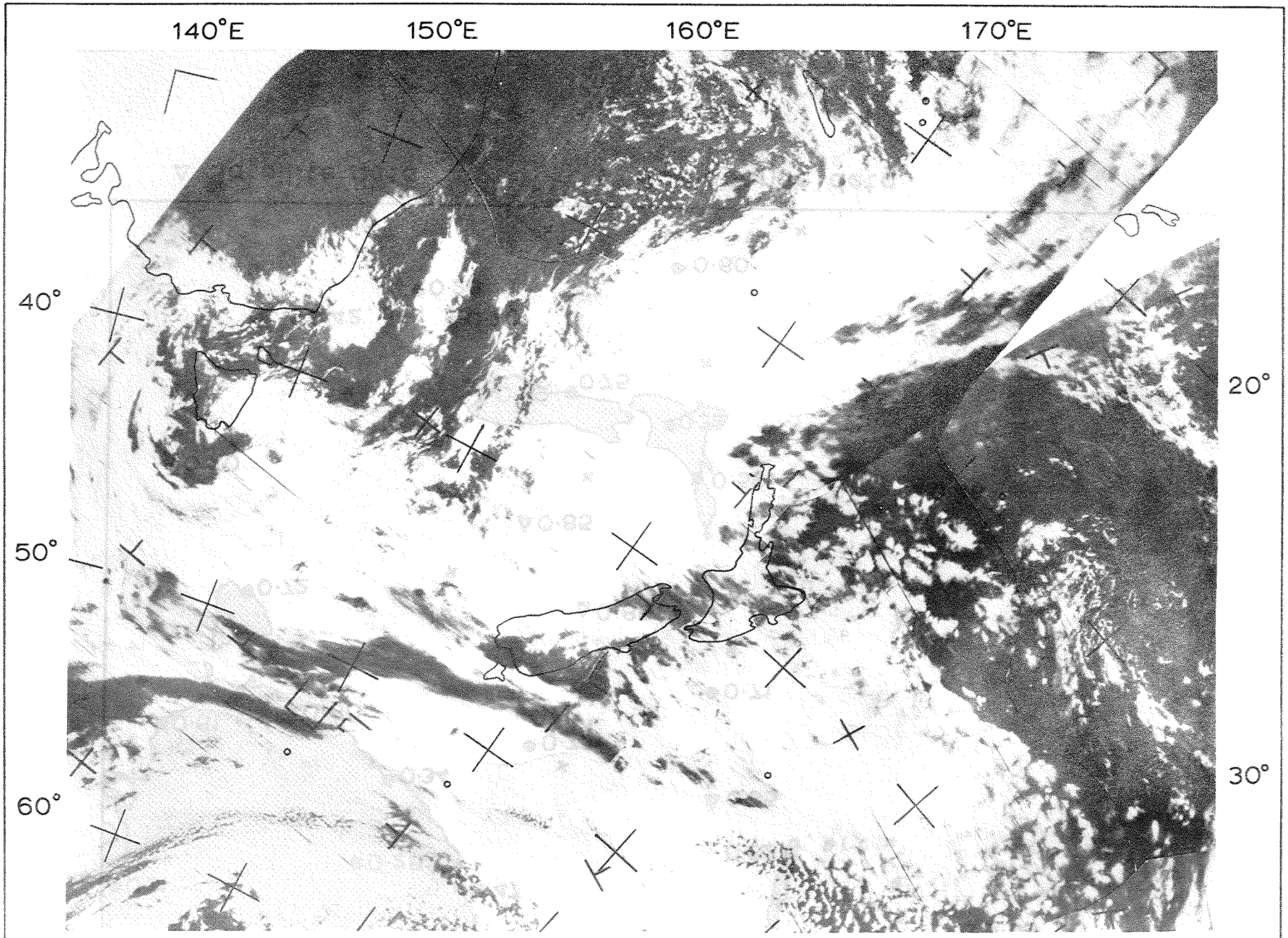

FIGURE 5: ESSA-8 MOSAIC FOR 3 JANUARY 1971

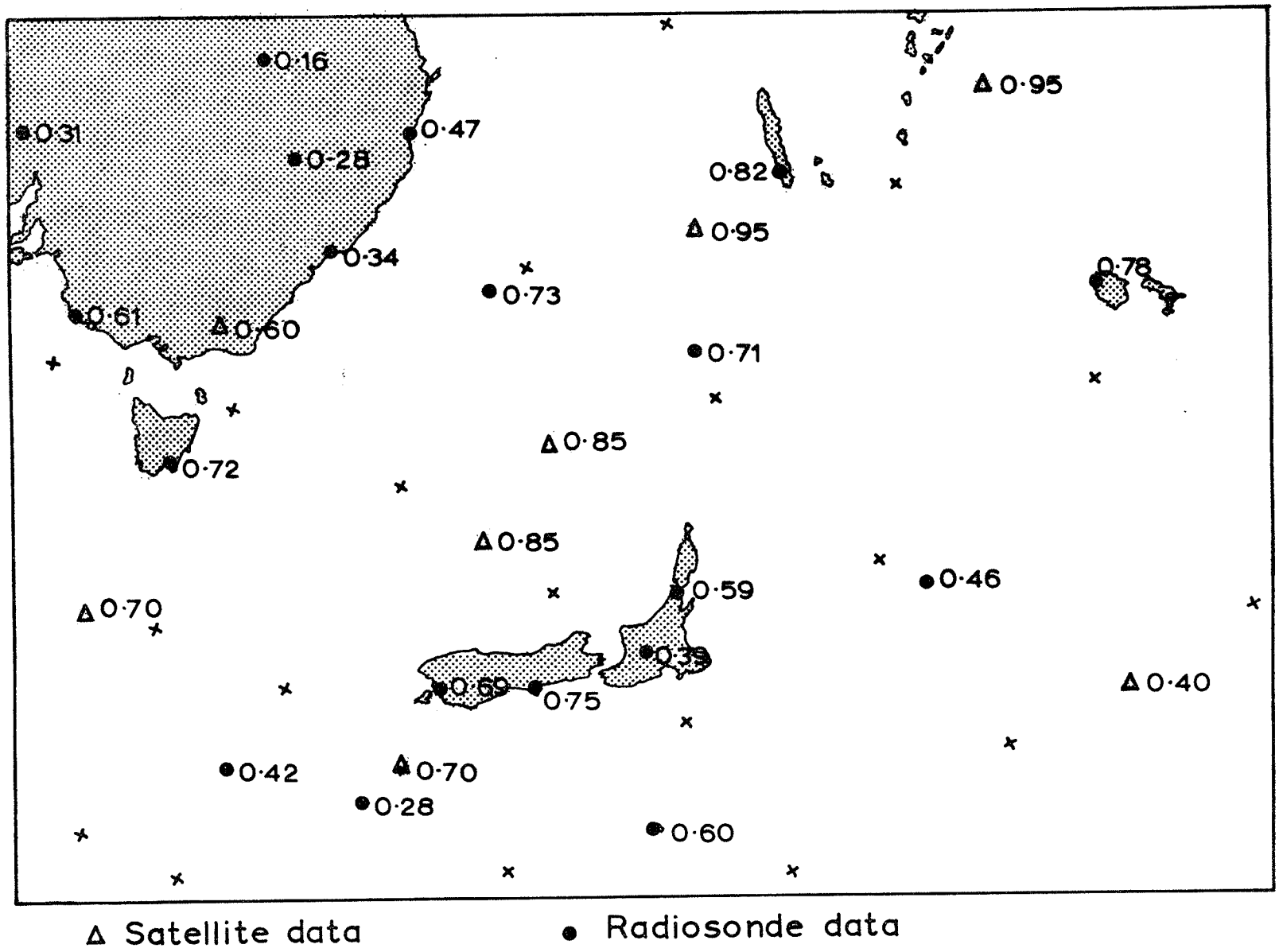

Fig. 6 Radiosonde and satellite derived mean relative humidities used for the 0000 GMT analysis on 2 January 1971.

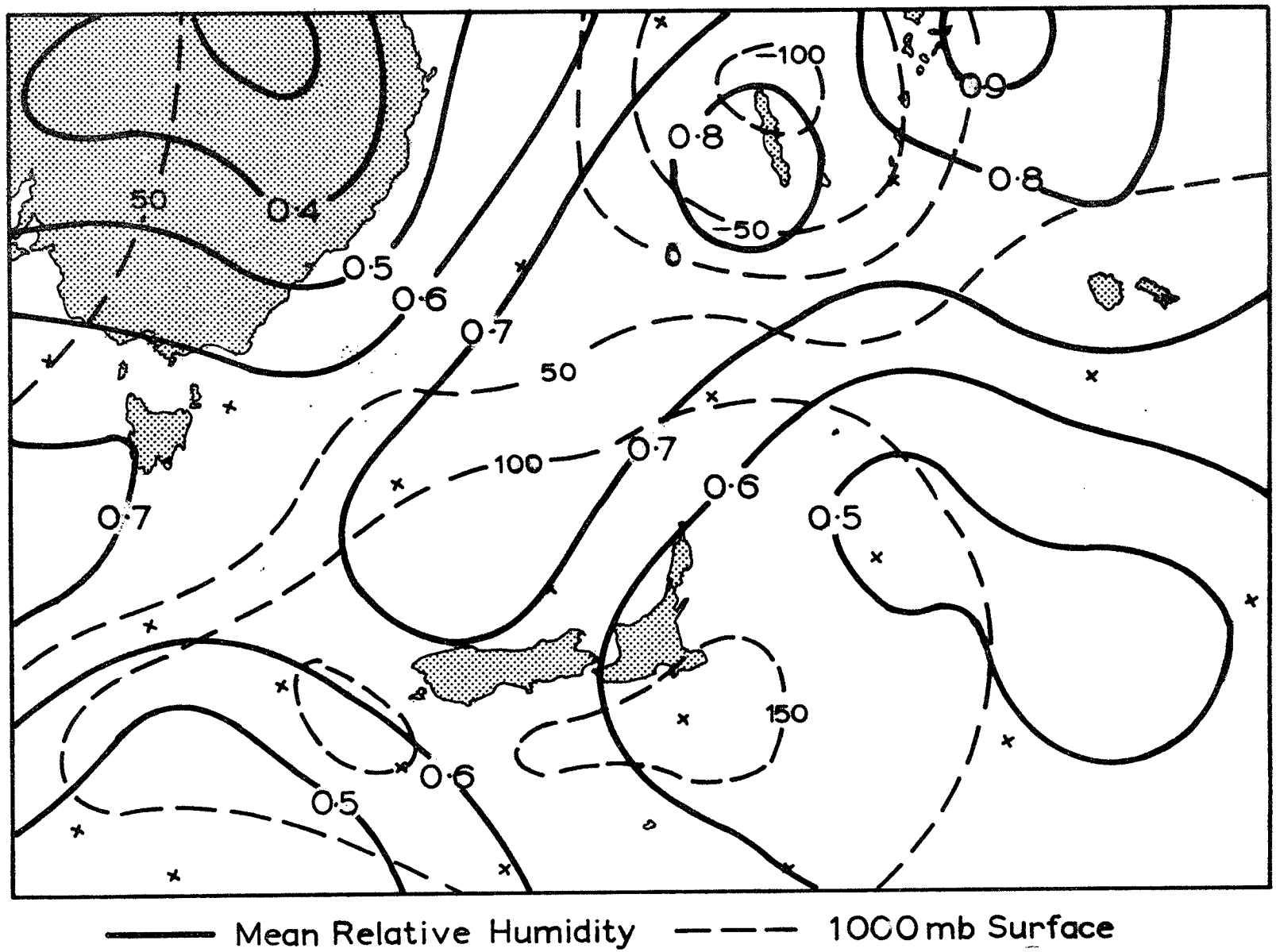

Fig. 7 The initial humidity analysis for 0000 GMT 2 January 1971.

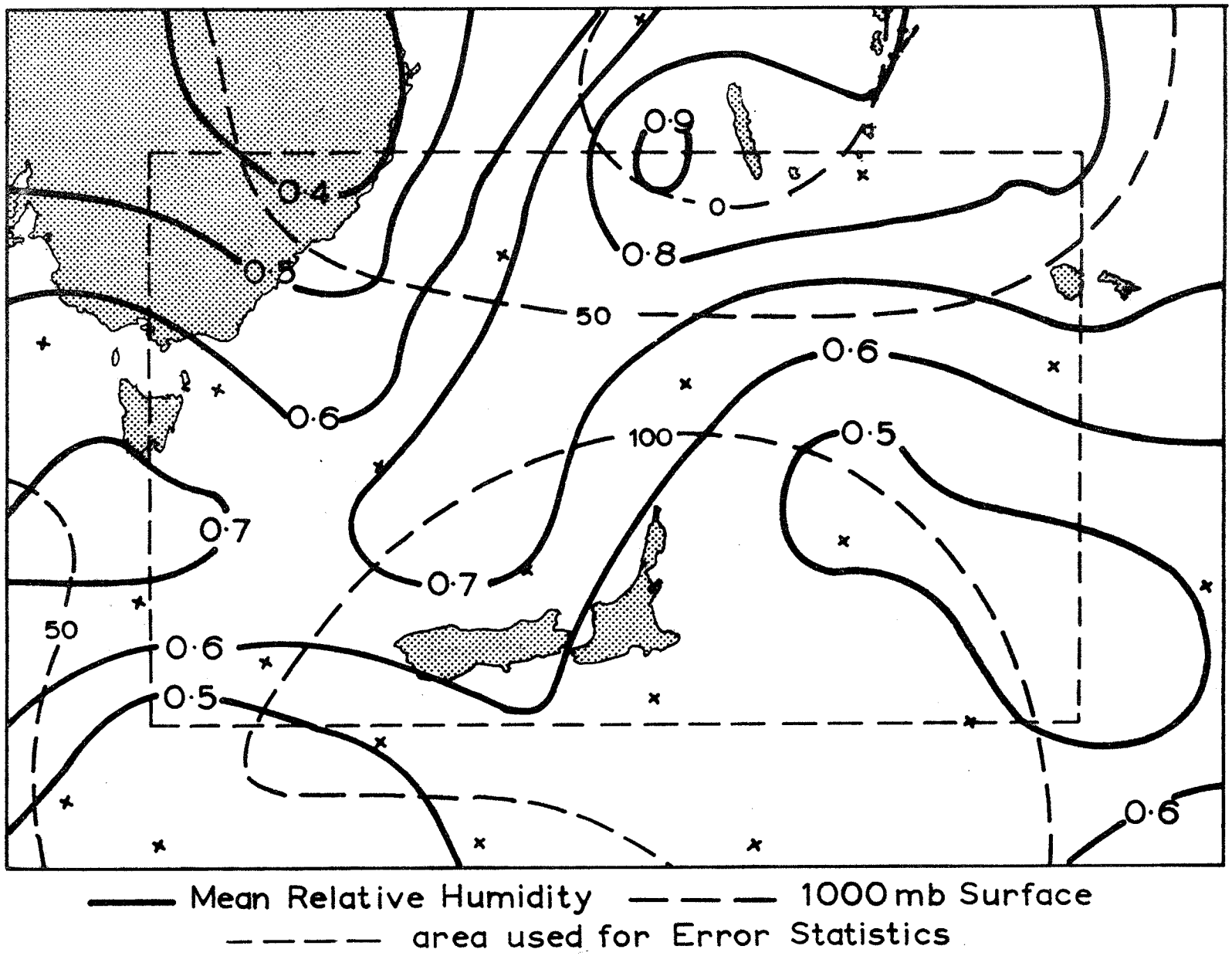

Fig. 8 The predicted 1000 mb height (dashed lines) and mean relative humidity (heavy lines) for 0000 GMT, 3 January 1971. The verification area is also shown in dashed lines.

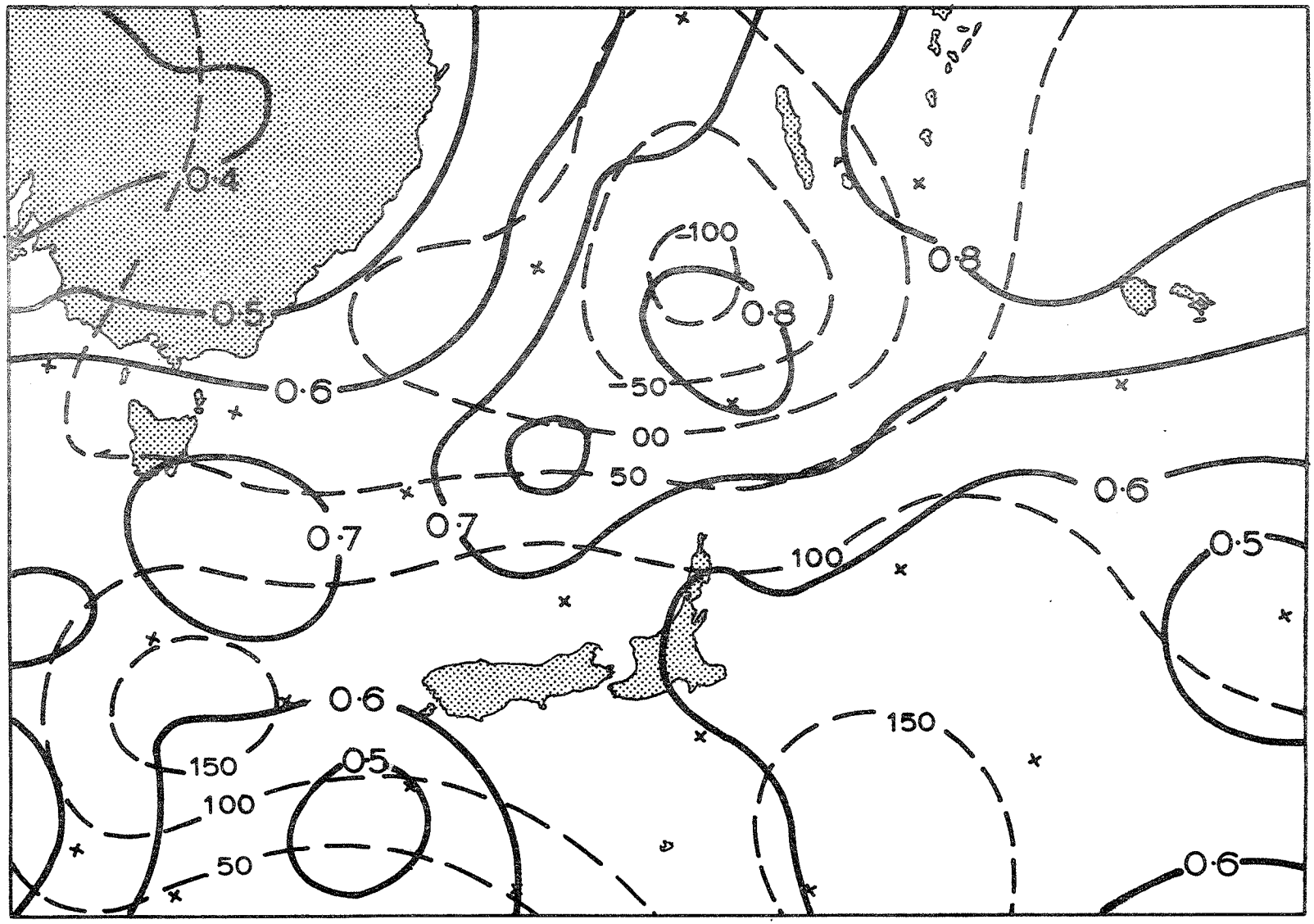

Fig. 9 Verification analyses of mean relative humidity and 1000 mb height for 0000 GMT 3 January 1971.

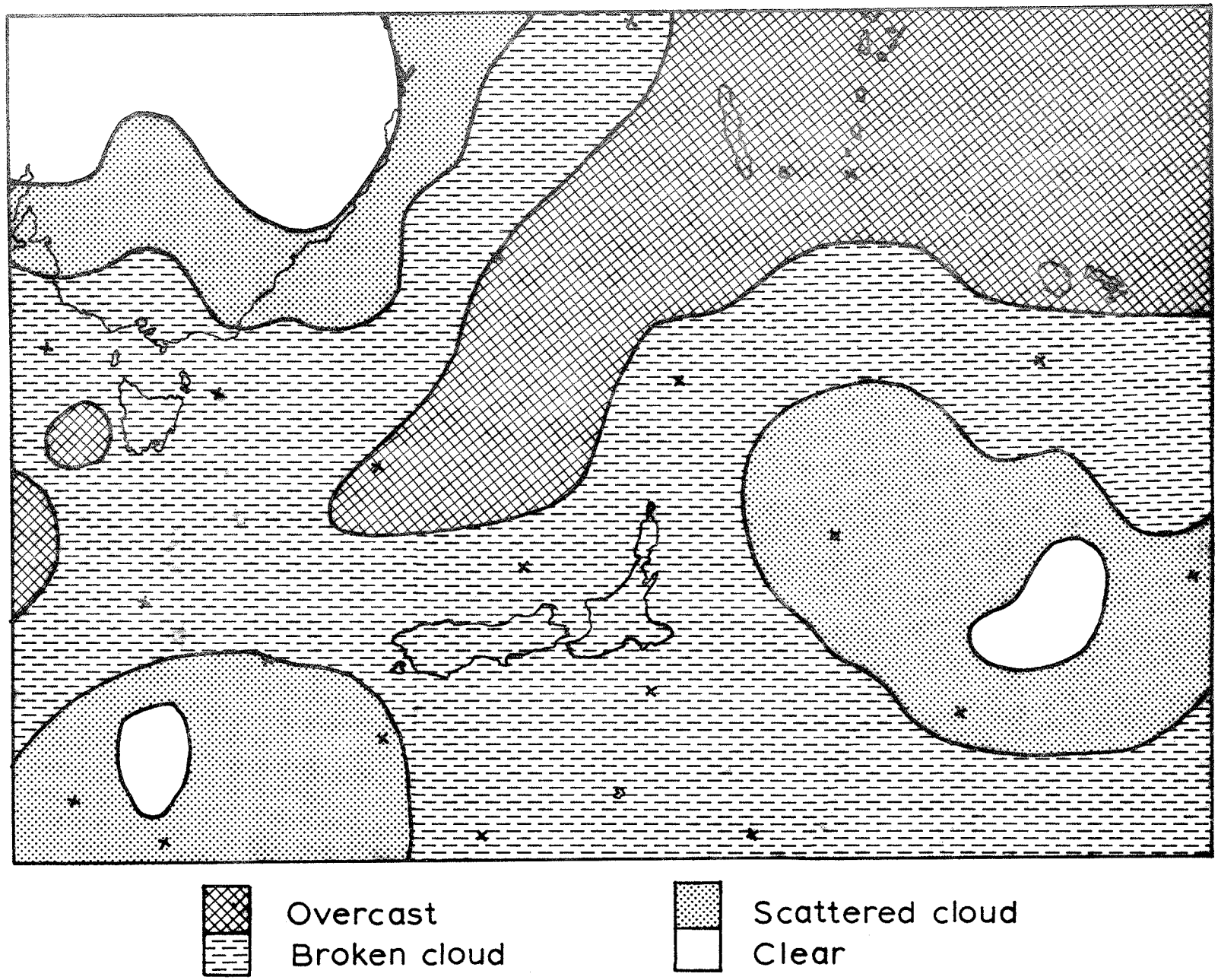

Fig. 10a Initial cloud cover analysis 0000 GMT, 2 January 1971.

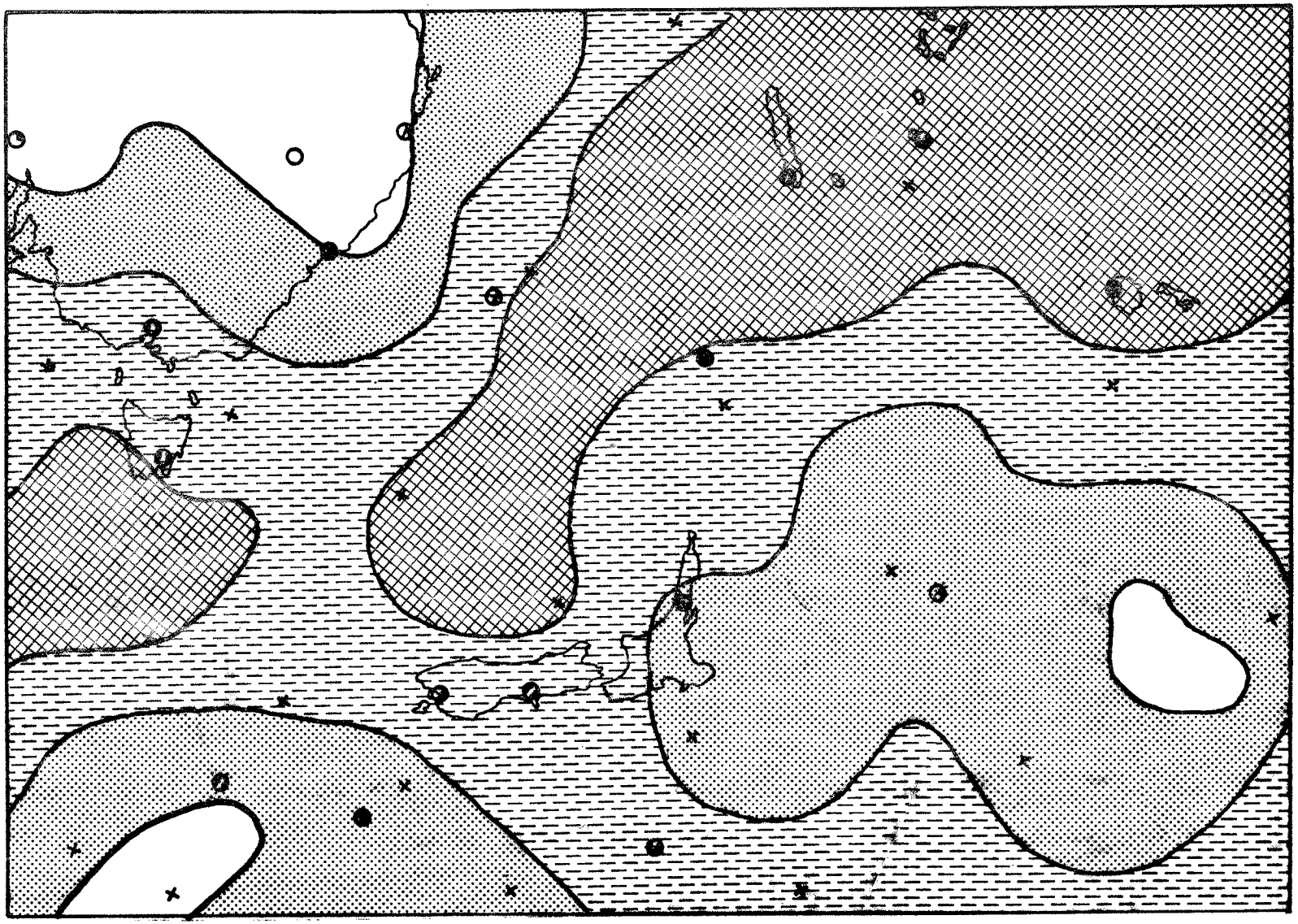

Fig. 10b Cloud cover predicted for 0000 GMT, 3 January 1971 with synoptic observations of total cloud cover. (legend as for Fig. 10a).

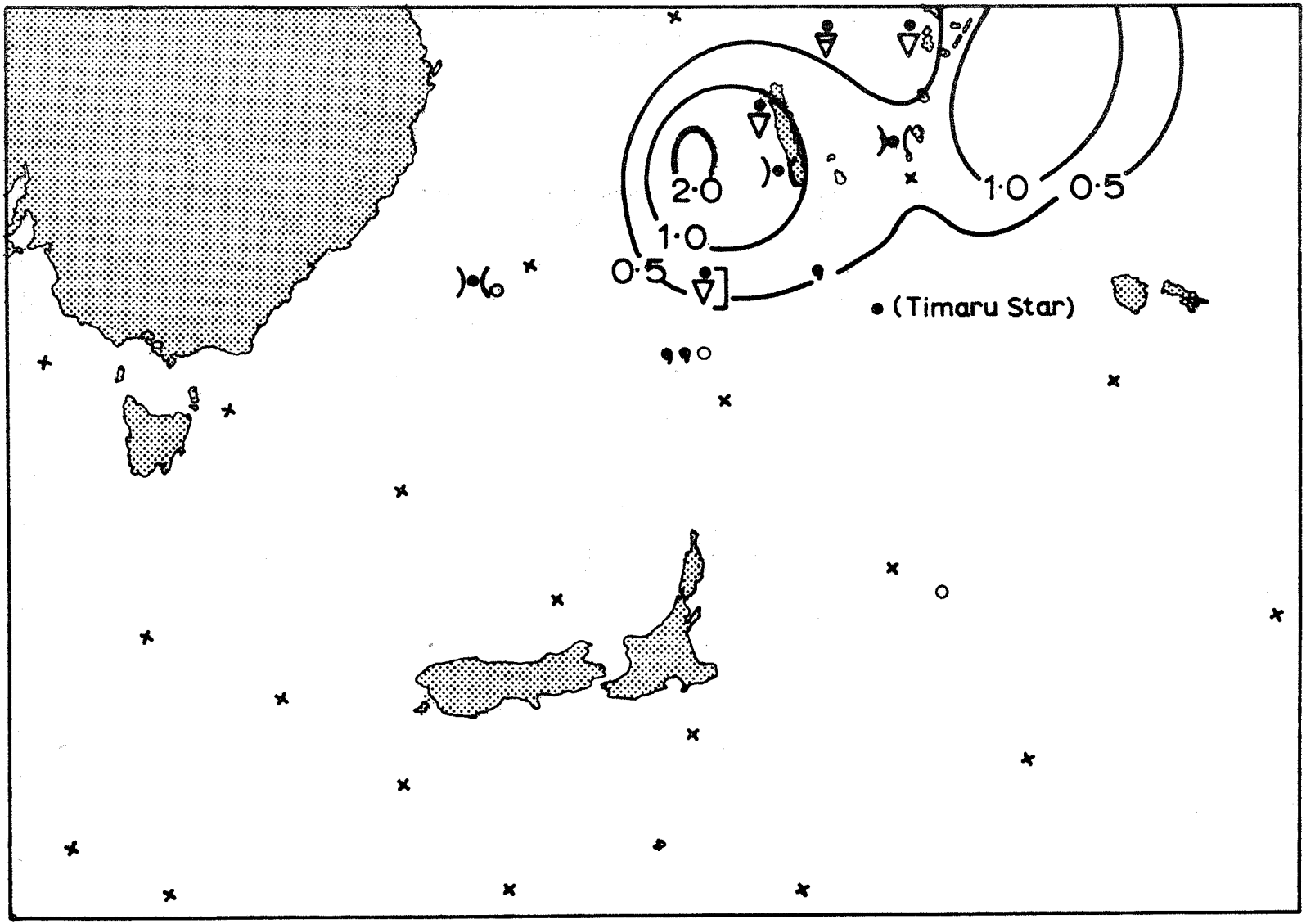

Fig. 11a Predicted rainfall rate in mm/hr for 0000 GMT, 3 January, 1971, together with synoptic observations showing precipitation.

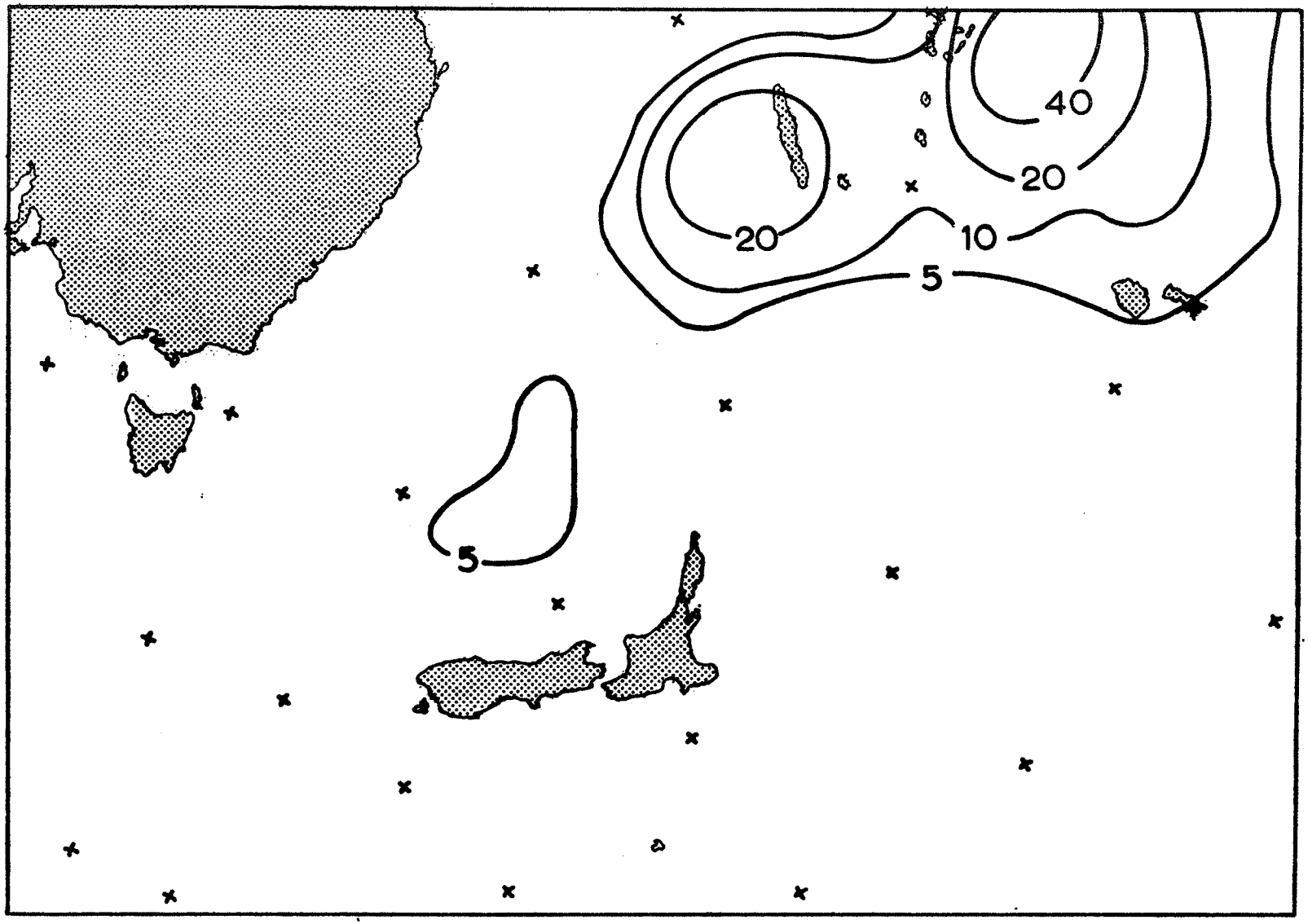

Fig. 11b Forecast of total rainfall (in mm) over the 24 hour period ending 0000 GMT, 3 January 1971.